Normal Vector Information Registration and Comparisons with Mutual Information

Xiahai Zhuang, and Lixu Gu, *Member, IEEE*

Abstract—We propose a new similarity measure for medical image registration and make comparisons with two kinds of mutual information (MI) methods in the literature. This new measure is computed from the normal vector information (NVI) of the images instead of pixel intensity that the MI methods based. The NVI of an image is extracted from the relationship between pixels and computed from the normal vector of the pixel based on their local isosurface. The NVI method has been proved to be able to successfully register two-dimensional (2D) images. In this paper, we will apply it in three-dimensional (3D) medical images and employ the known-result datasets to quantitatively evaluate the performances of the NVI and MI methods. The visual assessment is employed for the unknown-result clinical image dataset registrations. The results show that the NVI method is ready to be affected by the salt-and-pepper noise; while when the random noise is removed, the NVI method performs no worse than the MI methods.

I. INTRODUCTION

IMAGE registration is an enabling technology not only for image guided surgery and therapy in clinical applications, but also plays a vital role in many other biomedical applications [2]. It also addresses an essential problem needed to be solved in medical robotic applications and other techniques used in the operating room in the future [3]. In an image registration procedure, there is a need to find a geometric transformation that maps the given first image (or volume) into the reference with best similarity. A very critical component of the registration procedure is the choice of the similarity measure to evaluate how well the transformed image "matches" the reference. In [4], Penney *et al* had a survey of the similarity measures based on image intensity in the literature and made comparisons between them. Among those measures, mutual information (MI) seems to be better than other methods in multi-modality registration. Since its emergence in the middle of 1990s, many scientists have contributed to the development and acceptance of the MI method and the MI based method had been successfully applied in many kinds of registration tasks [6, 7, 8]. In this paper, we will employ a new similarity measure to register the 3D medical images and make comparisons with the two different MI methods in the literature to assess its performance. This new method is based on normal vector

(NV) information (NVI) of the images instead of intensity [1]. The NV in one image is the vector that is perpendicular to the local isosurface of one pixel in one image. As Fig. 1 shows, any pixel of the image has a value of intensity; then one can draw an isosurface or contour line from the image basing on the intensity value; and the NV is the vector perpendicular to the isosurface or contour line.
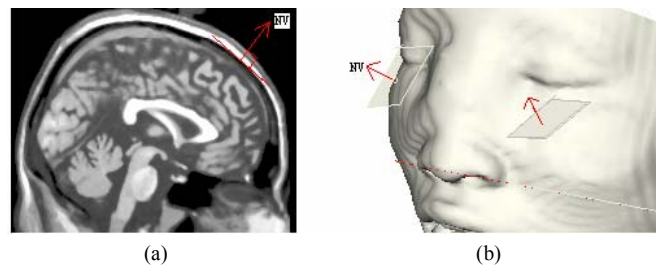

(a)   (b)

Fig. 1 Demonstration of the NVI. (a) NV in 2D image; (b) NV in 3D image.

This paper is organized as follow: in Section II, we present the criterion of the NVI similarity measure and the registration algorithm. In Section III, experiments to show the features of the NVI versus MI similarity measures will be presented; registrations results of the NVI and MI methods are offered for comparisons. Conclusions and discussions are given in Section IV.

II. NORMAL VECTOR INFORMATION SIMILARITY MEASURE

A. Why Can the NVI Measure Works

As Fig. 2 (a), (b) and(c) show, the PD, T1 and T2 MRI images of SBrain[1], differ in their grey value distribution but the respective NVI images of them are rather similar. Here each component of the normalized NV value is given value to each RGB color pigment when displaying a NV value. The vectors in opposite directions are regarded as the same because a vector and its direction plus 180 degree are considered as the same when computing similarity measure values. We could find in Fig. 2 (d), (e) that the CT NVI image is quite similar to the NVI image of the MRI image in those regions that CT image could catch the surface information, while in the center part of CT image the NVI image loses most of the information. To evaluate the similarity between CT and MRI images, it is feasible to account for those areas where both of the images have caught the surface information [1]. The definition of NVI similarity measure is based on this criterion.

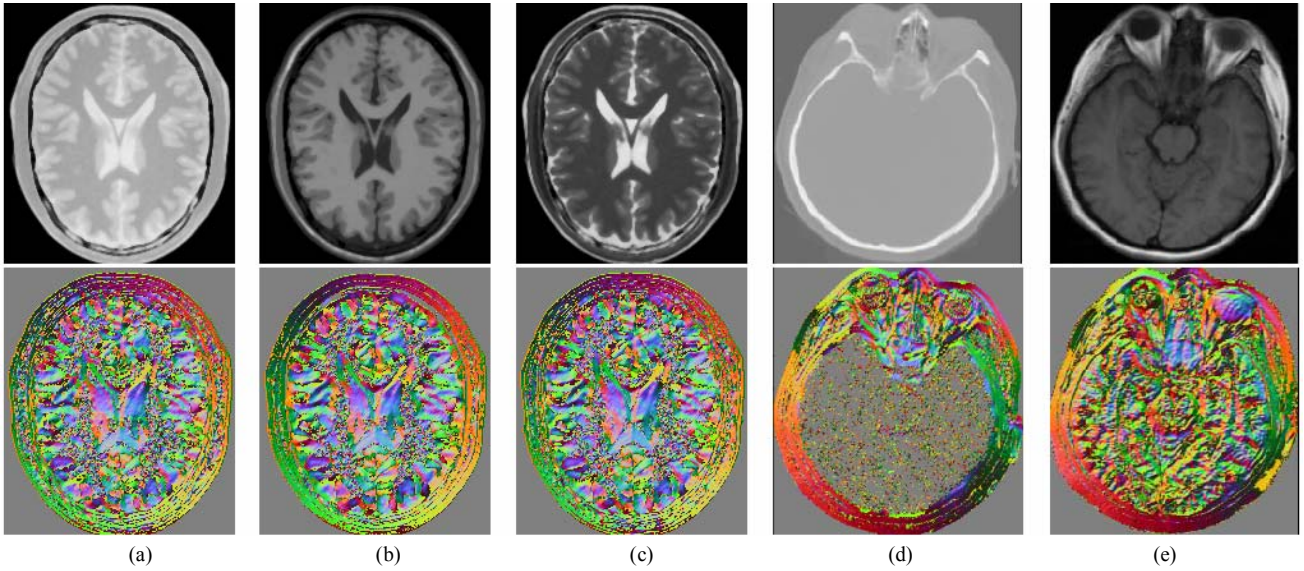[1]From Brainweb http://www.bic.mni.mcgill.ca/brainweb

Fig. 2 Different modalities of images and their respective NVI image contrast. Images of top row are 2D slices from medical image volumes; bottom group are the 2D slice from their respective NVI images. (a) from the PD MRI image; (b) from the T1 MRI image; (c) from the T2 MRI image; (d) from the clinical CT image; (e) from the clinical MRI image.

B. Definition

To evaluate the alignment between two images, a simple idea is to calculate how many locations the two images share the same NV value. It is feasible to calculate the same value of the vector but it would be too strict a criteria.

Here cosine of the included angle of two NV vectors is adopted to evaluate the similarity between two NV values. Then the average of all the square of cosine values of the NVI images could be a standard in evaluating how much the two NVI image are in similarity, which is how much the respective images are aligned. This method can exclude the problem that the two images have information at different scale in some regions such as the center part of the brain [1]. The NVI similarity measure algorithm between test image T and reference image R is defined as below:

$$S(T,R,g) = \frac{1}{|V|} \sum_{X \in V} \left[\cos\theta(N(X'), N(X)) \right]^2 \quad (1)$$

Where, S and g stand for the similarity measure value and the transformation, respectively. V is the sample volume from the test image; $N(X)$ denotes the NV value at location X in the transformed test image and $X' = g(X)$ is the location that pixel X in the test image mapped to the reference image by transform g. $N(X')$ is the NV value of location X' in the reference image. θ represents the included angle between the two corresponding vectors.

C. NV Value Computation

Isosurfaces represent the surfaces formed by those points in the image that have the same gray value. The NV of a location is a vector perpendicular to the isosurface as shown in Fig.1. The gradient vector of the gray values is the direction along which the intensity increases mostly. Then, the gradient vector of a gray value is perpendicular to the isosurface too

[9]. Therefore, we can employ the normalized gradient vector of gray value to compute the NV value. As the NV value can be drawn from the normalized gradient of image, the differentiability of the image modeling is acquired. A generic scheme is the cubic B-Spline image representation:

$$f(X) = \sum_i C_i \beta^{(3)}(X - X_i) \quad (2)$$

Where $\beta^{(3)}(X)$ is a differentiable convolution kernel given by the product of $\beta^{(3)}(x)\beta^{(3)}(y)\beta^{(3)}(z)$. This model is continuous, differentiable and serves our purpose in computing the image gradient to compute the NV value.

Another efficient method is to use discrete sample points on the lattice to linearly interpolate the derivative of the image:

$$\partial f / \partial X = (f(X_{+1}) - f(X_{-1})) / (X_{+1} - X_{-1}) \quad (3)$$

This method works efficiently especially when the spacing of the image is very close. Generally, the spacing between the slices of 3D medical images is too thick to use formula (3) to compute the NV. However, one can employ the B-Spline interpolation to resample the 3D image into the image with small slice spacing and then uses formula (3) to calculate the NV value. This method can obtain the same accurate NV value like using formula (2) while cost as little computation run time as that of using formula (3).

D. NV in the Transformed Image

One can easily imagine that the NV of those pixels in an image is changed when the image is transformed by a non-translation transformation. Hence, the NVs of the test image are not consistent during the registration process when the transformation applied to the test image is changing time to time. Assuming the transformation g is the combine of a rotation r and a translation l. The translation can not change the normal vector of the isosurface of the image; but when

applying the rotation r to the image, the normal vector is rotated the same angle (value) of r too. Therefore, the NV in the test image is computed as:

$$N(X) = N_s(X) \times r, \tag{4}$$

where, $N_s(X)$ is the NV value of pixel X in the test image when no transformation is applied to it, r is the rotation transformation matrix.

III. EXPERIMENTS

In our experiments, we firstly perform a series of tests to quantitatively compare the performance of the NVI method and two MI methods using the known-result datasets. The two MI methods are: the MI method employed in [6, 7] and the normalized mutual information (NMI) [8]. The MI method proposed in [5] is not concerned here because this method does not perform as well as other three methods in our experiments. Then, the clinical images will be employed to further confirm the conclusion drawn in the known-result experiments. The optimization, interpolation and transformation scheme are the regular step gradient descent optimizer, linear interpolation and rigid transformation respectively. In order to objectively evaluate the results, the optimization used in the three methods takes the same parameters in each experiment. The parameters of the two MI measure follow the advice in [10] and ITK[2] user menu. The MI method of [6, 7] and of [8] are marked as MI_M and NMI respectively for convenience. As for the sampling which determines the accuracy in evaluating the similarity, NIV and MI_M both sample 5-10% of the total pixels and NMI uses all pixels [10]. Our programs are based on a MS Visual C++ and run on a P-IV 2.60 GHz PC with 1.0GB main memory.
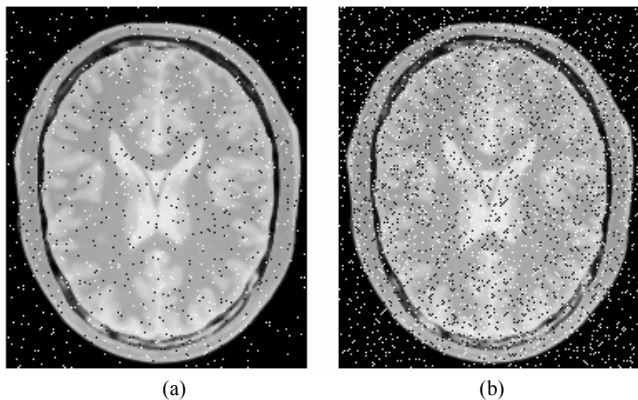

Fig. 3 The known-result registration datasets. (a) The 2D slices through 3D volume of PD MRI image with 3% salt-and-pepper noise added, and (b) the 2D slice of PD MRI image with 10% salt-and-pepper noise added.

A. Known-Result Registrations

The datasets used in this experiment are the PD and T1 MRI brain images downloaded from the Brainweb, which extent $181 \times 217 \times 181$ with voxel size of $1 \times 1 \times 1 mm^3$ (Fig. 2 a and b). In each registration, the test image is resampled into a misregistered image using a recorded rigid transformation T.

[2] http://www.itk.org

The parameters of T, such as translation with unit millimeter (mm) and rotation with unit angular degree (0~360), are randomly given value within a given range. Here, two groups of registrations are tested; one uses the range of 10-20 for the parameters, the other is 20-30. Each registration will record the parameters before and after the registration, including the average displacement of T before registration: ϖ_B, the run time: TIME, and the average Euclidean Distance of misalignment (ϖ_R) after registration:

$$\varpi_R = \frac{1}{|V|} \sum_{X \in V} \| g(X) - T^{-1}(X) \|, \tag{5}$$

where, V denotes the test image volume, g represents the registration result transformation; T^{-1} is the inverse transformation of T and $\| \|$ stands for the Euclidean Distance.

The NVI and MI_M sample 5% pixels of the image in their registration. As table. 1 and table. 2 show, in each group, the different registration method will register the random initially transformed test image of non-noise added, 3% salt-and-pepper noise added (fig. 3 a) and 10% noise added images (fig. 3 b) for 50 times. Column ϖ_B gives the average initial displacement of 50 times; column ϖ_R and column TIME record the average displacement and run time of the successful registrations; SUC stands the probability of success from the 50 registration cases.
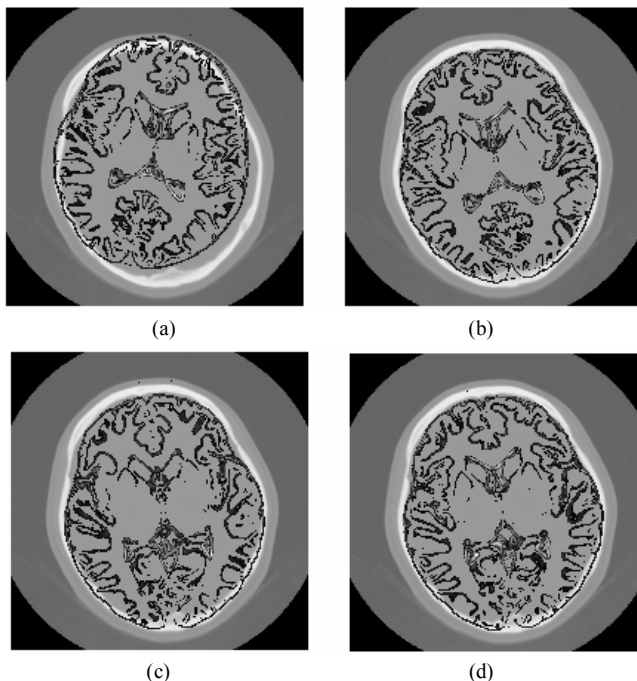

Fig. 4 Demonstration of a typical result of clinical CT-MRI datasets registration. The 2D slice through 3D volume of MRI contour line overlays CT before registration (a), after registered by the NVI method (b), after registered by MI_M (c), and after registered by NMI (d).

B. Unknown-Result Registrations

In this section, five sets of clinical images of CT and MRI will be employed in the NVI, MI_M and NMI registrations. These images were provided by Shanghai East Hospital. The

CT images were scanned by a GE CT scanner with size of $512 \times 512 \times 32$ and voxel spacing $0.44 \times 0.44 \times 3.75$ (mm). The MRI images were scanned by a Philips scanner in size of $256 \times 256 \times 100$ with spacing $0.70 \times 0.70 \times 1.00$ (mm) or size $512 \times 512 \times 32$ with spacing $0.45 \times 0.45 \times 4.00$ (mm). All the images are recast to pixel value ranging from 0 to 0x0fff, extends $201 \times 201 \times 101$ with spacing $1 \times 1 \times 1$ mm.

In order to achieve good accuracy of the NVI and MI_M methods, we sample 10% pixels of the image in this section. As the results turn out, the three methods all succeed in the five examples, which is visual assessment. Fig. 4 gives a typical result of the registrations; the results of the NVI (fig. 4 b) and NMI (fig. 4 d) seem to be better than that of MI_M (fig. 4 c). The average run time of the five registrations for the NVI, MI_M and NMI are 275, 248, and 1006 seconds respectively.

TABLE.1
PD-T1 IMAGES REGISTRATIONS (50TIMES) FOR IMAGE WITHOUT RANDOM NOISE ADDED, 3% SALT-AND-PEPPER NOISE ADDED AND 10% NOISE ADDED IMAGE DATASETS. 10~20 MEANS THE PARAMETERS OF THE RIGID TRANSFORMATION RANGE FROM 10 TO 20, $\overline{\varpi}_B$ AND $\overline{\varpi}_R$ STAND THE AVERAGE DISPLACMENT BEFORE AND AFTER REGISTRATION. TIME IS THE AVERAGE RUN TIME COMSUMED AND SUC GIVES THE SUCCESS REGISTRATION PROBABILITY.

10~20	Noise	$\overline{\varpi}_B$ (mm)	$\overline{\varpi}_R$ (mm)	TIME (s)	SUC
NVI	0%	41.16	0. 7245	137.8	100%
	3%	43.38	0. 7480	145.6	82%
	10%	42.02	1.111	152.8	24%
MI_M	0%	45.12	0.7791	111.6	100%
	3%	42.81	1.227	136.0	100%
	10%	42.02	1.443	207.9	70%
NMI	0%	44.84	0.8259	1262	100%
	3%	43.38	1.279	1276	100%
	10%	44.05	1.496	1235	100%

TABLE.2
PD-T1 IMAGES REGISTRATION (50TIMES)

20~30	Noise	ϖ_b (mm)	ϖ_r (mm)	TIME (s)	SUC
NVI	0%	73.66	0.7474	206.3	100%
	3%	72.81	0.8756	236.0	44%
	10%	71.49	1.223	256.1	10%
MI_M	0%	73.19	0.7695	145.7	92%
	3%	70.12	1.259	188.0	70%
	10%	72.61	1.537	236.7	30%
NMI	0%	72.30	0.8508	1500	100%
	3%	73.71	1.247	1520	100%
	10%	71.92	1.539	1568	100%

IV. CONCLUSION

Tabel. 1 and 2 both demonstrate that the NVI method does not perform as well as the two MI base methods in the noised images registrations -- its SUC value decreases greatly when the noise is added, while the two MI methods are affected less. This is reasonable because the NV computation using formula (3) employs 6 pixels' intensity in 3D images; if the interpolation accuracy probability of pixel intensity is p, then in 3% noised image, the accuracy probability of NV computation is $p*(1-3\%)^6 = 0.83p$, and $p*(1-10\%)^6 = 0.53p$ in 10% noised image. However, when the tested images are very

"clear", that is without random noise added the NVI method gets full percent of success probability in the two groups of experiments, and the average accuracy of the success registrations of the NVI is better than the two MI methods. The MI_M method seems to be most efficient in run time and it performs not so well when the displacement is huge. The NMI method succeeds in all the registration tasks but it also consumes more time because it employs all the pixels in the images to compute its value. In the unknown-result experiments, the clinical datasets are in high image quality after process of noise filter. The NVI achieves better accuracy than MI_M and costs less run time than NMI. All the three methods are successfully register the five datasets. In our future work, we will compare these methods in nonrigid registration examples and discuss the influence of the different optimization methods.

REFERENCES

[1] Xiahai Zhuang, Lixu Gu, and Jianfeng Xu, *"Medical Image Alignment by Normal Vector Information,"* Y. Hao et al. (Eds.): CIS 2005, Part I, LNAI 3801, pp. 890 – 895, Springer-Verlag Berlin Heidelberg, 2005.

[2] David J. Hawkes, Dean Barratt, Jane M. Blackall, Adam G. Chandler, Jamie McClelland, Graeme P. Penney, "*Computational Models In Image Guided Interventions,"* in Proceedings of the 2005 IEEE EMBC, Page(s): 7246 – 7249, Shanghai, China, September 1-4, 2005.

[3] Kevin. Cleary, *"Medical Robotics and the Operating Room of the Future,"* in Proceedings of the 2005 IEEE EMBC, Page(s): 7250-7253, Shanghai, China, September 1-4, 2005.

[4] G. P. Penney, J. Weese, J. A. Little, P. Desmedt, D. L. G. Hill, D. J. Hawkes, *"A comparison of Similarity measures for use in 2-D-3-D medical image registration Medical Imaging"*, IEEE Transactions on Volume 17, Issue 4, Page(s):586 – 595, Aug. 1998

[5] P. Viola and W. M. Wells III, *"Alignment by maximization of mutual information,"* in Proc. 5th Int. Conf. Computer Vision, Boston, MA, pp. 16–23, June 20–23, 1995.

[6] David Mattes, David R. Haynor, Hubert Vesselle, Thomas K. Lewellen, and William Eubank, *"Pet-CT Image Registration in the Chest Using Free-form Deformations,"* IEEE Ttrans on Medical Imaging. vol.22, no.1.Jan. 2003.

[7] Philippe Thévenaz and Michael Unser, *"Optimization of Mutual Information for Multiresolution Image Registration,"* IEEE Trans on Image Processing, vol.9, no.12, Dec. 2000.

[8] J. Hajnal, D. J. Hawkes, and D. Hill. *Medical Image Registration*. CRC Press, ch.3, 8.5, 8.10.6, 2001.

[9] K.H. Hoehne and R. Bernstein, *"Shading 3D-Images from CT Using Gray-Level Gradients,"* IEEE Trans. Medical Imaging, Vol. MI-5, No. 1, pp. 45-47, March 1986.

[10] Lydia Ng, *"Overview: ITK Registration Methods,"* SPIE2004: Medical Image Segmentation and Registration With ITK, 2004.